Plasma etching of sputtered Mo and $MoSi_2$ thin films in NF_3 gas mixtures

T. P. Chow
General Electric Company, Corporate Research and Development, Schenectady, New York 12301 and Rensselaer Polytechnic Institute, Center for Integrated Electronics, Troy, New York 12181

A. J. Steckl
Rensselaer Polytechnic Institute, Center for Integrated Electronics, Troy, New York 12181

(Received 27 January 1982; accepted for publication 16 April 1982)

Plasma etching characteristics of sputtered molybdenum and $MoSi_2$ thin films using various NF_3 gas mixtures in a planar reactor are presented. Anisotropic (vertical-to-lateral etch ratio of ~ 3) edge profiles were obtained. The etch rates of Mo, $MoSi_2$, doped poly-Si, and SiO_2 were determined as a function of rf current, reactor pressure, and NF_3 concentration. At 1 A and 100 mTorr in 100% NF_3, etch rates of 2490, 3440, 14000, and 670 Å/min were measured for Mo, $MoSi_2$, doped poly-Si, and SiO_2, respectively. Also, the etch rate ratios of Mo, $MoSi_2$, doped poly-Si over SiO_2 were 1.5–4, 4–8, and 12–24, respectively. Diluting the NF_3 plasmas with argon or helium decreased the etch rates for all the materials studied here. At 200 mTorr and 1 A, the Mo etch rate dropped from 1800 Å/min in 100% NF_3 to 540 Å/min in 20% NF_3/80% Ar, while the corresponding silicide etch rate decreased from 7850 to 1130 Å/min. Auger spectroscopy measurements inferred that the desorption of molybdenum products, but not the silicon ones, may be the rate-limiting step in the etching process. Furthermore, dc voltage measurements on the rf electrode indicated a higher degree of ion bombardment at low pressures (< 150 mTorr) and in NF_3 plasmas diluted with inert gases.

PACS numbers: 52.40.Hf, 81.60. – j, 52.75. – d

I. INTRODUCTION

Refractory metals and metal silicides are recently under active development for use as gate and interconnection materials in very large scale integrated (VLSI) circuits.[1–9] The main advantage of these materials over conventional doped polycrystalline silicon (poly-Si) is their high conductivity. Since it has become apparent that scaling down of devices may not lead to overall higher circuit performance unless the constraint imposed by the interconnects is relaxed, these materials are becoming an integral part of most VLSI processes.

Various dry etching methods, such as planar plasma etching and reactive ion etching, are widely used to define small dimensional structures. Whereas dry etching of poly-Si using flourine- or chlorine-based gases have been extensively investigated,[10–15] relatively little work has been reported for the refractory metals and metal silicides. Most of the work reported on these materials is confined to flourocarbons, such as CF_4/O_2 [1,4–6,9,16–18] even though etching with NF_3,[19] SF_6,[20] and CCl_4/O_2 [21,22] have been reported. In this paper, the plasma etching characteristics of sputtered molybdenum and molybdenum disilicide thin films using various nitrogen trifluoride gas mixtures are presented. In particular, the effects of rf current, reactor pressure, and dilution with inert gases (argon and helium) on the etching process have been studied and compared with those of silicon dioxide and phosphorus-doped poly-Si.

This paper is organized as follows. The experimental procedure is described in detail in Sec. II. The edge profiles of $MoSi_2$, Mo, and $MoSi_2/n^+$ poly-Si ("polycide") are shown in Sec. III. Also presented in the section are the etch rates of Mo, $MoSi_2$, doped poly-Si, and SiO_2 versus rf current, reactor pressure, and NF_3 concentration. Furthermore, the dc voltage measured on the rf-coupled electrode under various conditions are described. In Sec. IV, the results are discussed in analogy to other fluorinated plasmas, particularly CF_4. Auger spectra are also presented and commented on. Finally, in the last section, the results of the present process are summarized.

II. EXPERIMENTAL PROCEDURE

The planar plasma reactor used was a commercial reactor (ETE Plasmafab), shown schematically in Fig. 1. The water-cooled electrodes have an outer diameter of 23.5 in. (60 cm) with the top electrode having an opening of 4 in. (10 cm) through which the etching gas was introduced into the chamber via a ceramic tubing of 0.25 in. (0.64 cm) in diameter. The rf power (380 KHz) was capacitively coupled to the top electrode. The bottom electrode as well as the chamber walls were grounded. The power applied is characterized in terms of rf current. The interelectrode spacing was set at 2.75 in. (7 cm) and the pumping speed at 475 cm^3/min. Both remained fixed throughout the experiment. The reactor pressure was changed by adjusting the flow rate only. The pressure range studied was between 80 and 250 mTorr with the corresponding flow rate between 20 and 80 cm^3/min. The residence time of the gas was estimated to be 30 sec. Hence, the system can be considered as a long residence time system. The top and bottom electrodes are made of titanium alloys while the chamber walls are stainless steel. The volume of the chamber was ~ 100 liters and the area ratio of the excitation electrode to the grounded surfaces was ~ 5. The wafers were placed at the periphery of the bottom electrode and 2-in.-diam wafers were used in the present study. All of the mixed gases were delivered to the reactor from precalibrated cylinders. All percentages mentioned in the text were the volume percentage at the inlet.

 0021-8979/82/085531-10$02.40

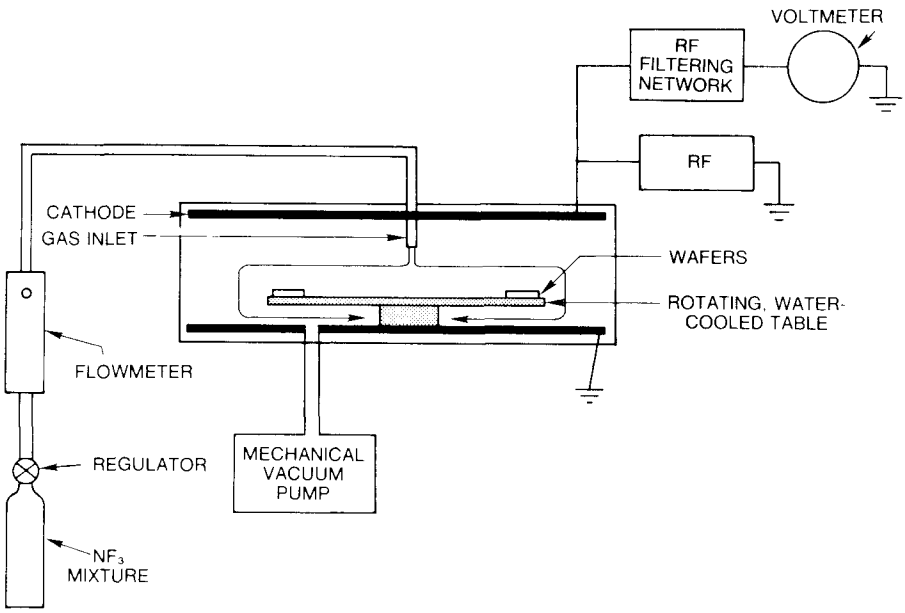

FIG. 1. Schematic diagram of the planar plasma etcher (ETE Plasmafab) used in this study.

Both molybdenum and molybdenum disilicide films were dc magnetron sputtered onto oxidized silicon substrates in a planar system system (MRC 603). The hot-pressed silicide target was stoichiometric in composition (Si/Mo~2). Deposition was done at room temperature for $MoSi_2$, but for Mo, a preheating step at 300 °C was performed for 5 min to ensure good adhesion. All the etching was done on the as-deposited films. Typical sputtering parameters were 1–3 KW of power and 3–10 mTorr of argon pressure. Silicon dioxide samples were made in steam at 1000 °C. Poly-Si samples were deposited in a low-pressure CVD system at 630 °C and subsequently doped at 1000 °C with $POCl_3$.

To determine the etched thickness of various samples, two different methods were used. Positive photoresist-(Shipley AZ1470) was used as the masking material for the Mo, $MoSi_2$, and doped poly-Si samples. An array of circular dots, 30 mil in diameter, was defined in a lithographic step. After etching, the resist was removed in acetone and the height of the etched step was measured with a Dektak profilometer. The second method, which was used for the oxide samples only, required no photoresist. Ellipsometry using a Rudolph Research/Auto-El was performed before and after etching. The etching process took place at room temperature for durations up to 5 min. The error bar indicates the average deviation.

To determine the degree of anisotropy, which is defined as the ratio of vertical to lateral etched depths, very narrow (1–2 μm) and long lines were defined with either projection or contact photolithography. Samples were cleaved and their cross sections were examined with scanning electron microscopy (SEM) before and after etching. To detect the adsorbed gas species, Auger Electron Spectroscopy (AES) was employed with a Physical Electronics SAM-545 Auger analyzer. Depth profiling was achieved by combining AES with argon ion milling. These measurements were not taken *in situ* in the etcher. Also, the dc bias on the powered electrode was measured through a LC filtering network. Immediately upon the application of rf power, the dc voltage observed on the rf electrode jumped to its peak value. As the etching progressed, the voltage fluctuated and gradually assumed a lower value. This dc voltage was monitored under various etching conditions to infer the degree of in bombardment on various surfaces. The voltage values mentioned below are the average of the peak and bottom values detected during etching.

III. RESULTS

To examine the line edge profiles, cross sections were examined under SEM. Figure 2 is a SEM photograph of a ~1 μm $MoSi_2$ line that was etched in NF_3 at 1 A and 100 mTorr. The 3000-Å-thick film was on oxidized silicon substrate. In this case, the photoresist was defined with a contact printer, resulting in a vertical ($> 80°$) resist sidewall. The

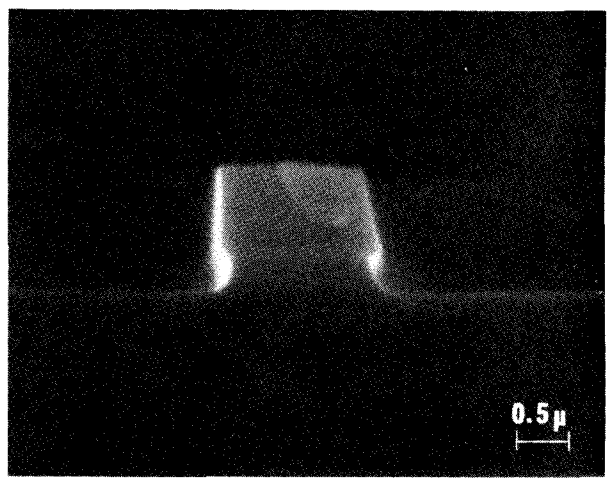

FIG. 2. SEM cross-sectional view of a ~1 μm $MoSi_2$ line which was etched in 100% NF_3 at 1 A and 100 mTorr. The ~1-μm-thick positive photoresist that was used as mask has not yet been removed. The 3000-Å-thick silicide film was deposited on oxidized silicon substrate.

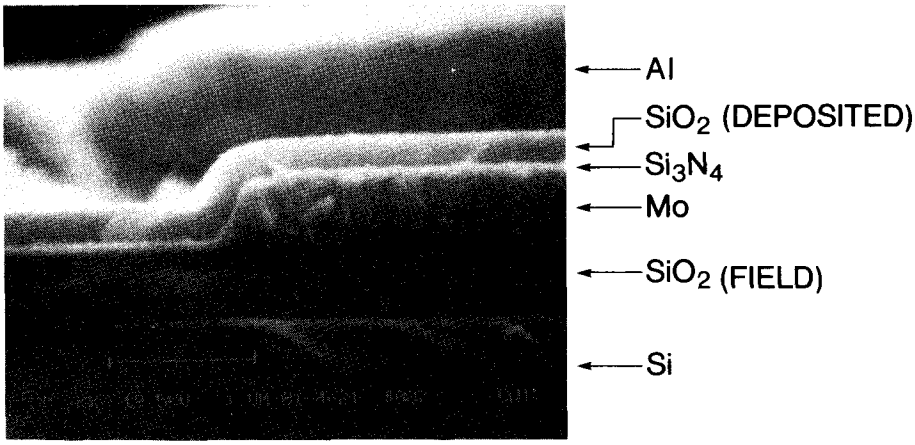

FIG. 3. SEM picture of an edge profile of a 3000-Å-thick Mo film which was etched in 100% NF_3 at 1 A and 200 mTorr. The resist has been removed and various layers of thin films (as indicated) have been deposited over the Mo layer.

anisotropy of the etched profile was ~3. Similar edge profiles were obtained for molybdenum films, as illustrated in Fig. 3. Here, the resist has been stripped and various thin films (Si_3N_4, etc.) have been deposited over the molybdenum layer. The anisotropy was also ~3. In Fig. 4, the edge profile obtained for a polycide structure is shown. The polycide stack had 3000 Å of $MoSi_2$ on 1500-Å-doped poly-Si. The photoresist was exposed in a projection aligner, which gave a more gradual (~60°) resist sidewall than the previous case. The anisotropy measured was again ~3. However, the poly-Si layer underneath the silicide was etched isotropically, leaving a silicide "roof" over the poly-Si. This feature of polycide etching is undesirable because of the difficulties in step coverage and linewidth control. A number of solutions to this problem have been implemented.[17,18,20,22,23] In particular, reactive ion etching of $MoSi_2/n^+$ poly-Si in CCl_4/O_2 and CCl_4/N_2 plasmas appears to be the most promising.[23]

To characterize in detail the NF_3 etching process, the etch rate was determined as a function of rf current, ambient pressure, and percentage of argon or helium in NF_3. In Fig. 5, the etch rate versus rf current is shown for 100% NF_3 at a pressure of 100 mTorr. The current range studied was between 0.6 and 2 A. Exceedingly high etch rates ($> 1\ \mu$m/min) were measured for heavily doped poly-Si over the entire

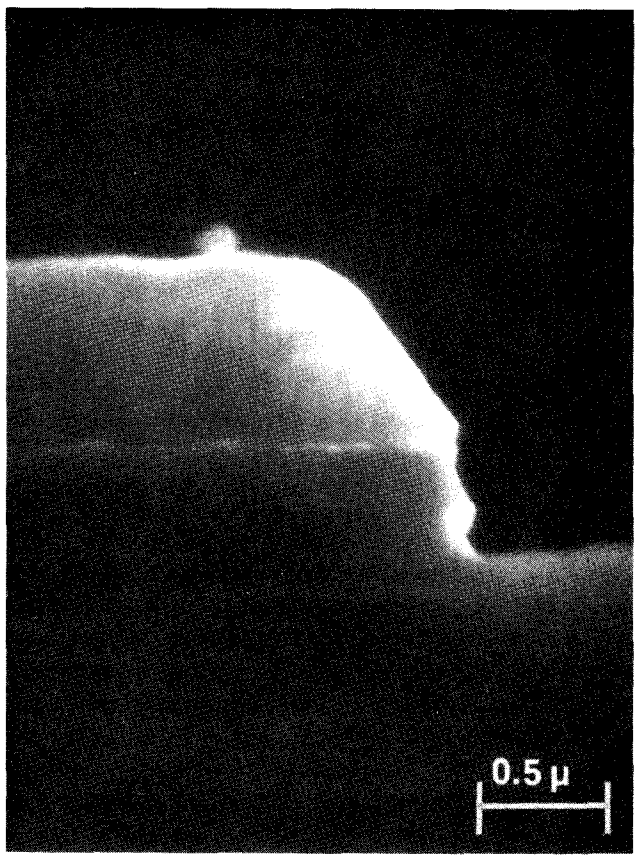

FIG. 4. SEM cross-sectional view of a $MoSi_2/n^+$ poly-Si ("polycide") stack which was etched in 100% NF_3 at 1 A and 100 mTorr. The ~1-μm-thick resist has not yet been removed. A silicide "roof" resulted from the isotropic etching of the underlying poly-Si and is readily observable. The substrate was oxidized silicon.

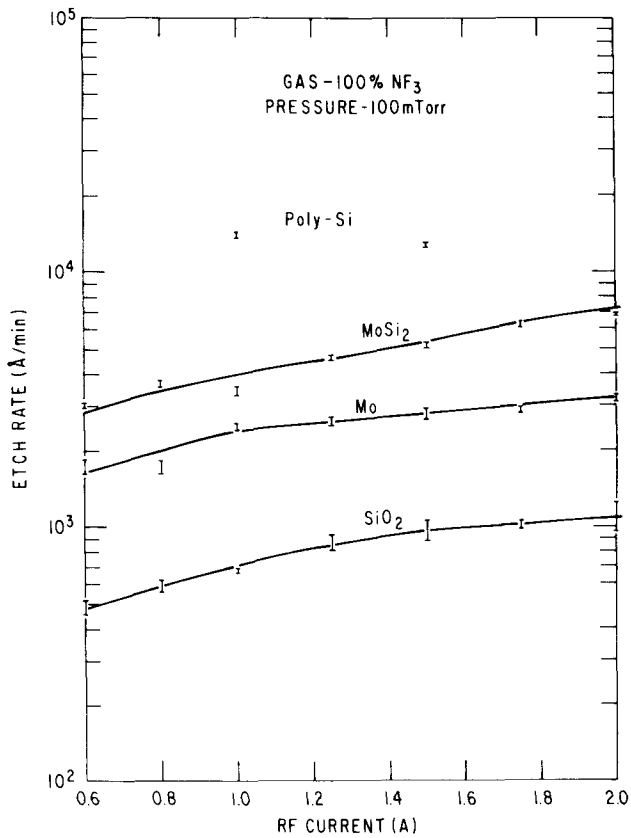

FIG. 5. Etch rates of Mo, $MoSi_2$, doped poly-Si, and SiO_2 are shown as a function of rf current at 100 mTorr in 100% NF_3.

current range. Generally, the etch rate of $MoSi_2$ was found to be higher than that of molybdenum, which in turn was higher than that of silicon dioxide. Also, in each case, the etch rate was increased monotonically with rf current. In particular, the silicide etch rate increased from 3000 Å/min at 0.6 A to 6800 Å/min at 2 A, while the corresponding ranges for molybdenum and SiO_2 were 1730–3200 Å/min and 450–1100 Å/min, respectively.

The dependence of the etch rate on the ambient pressure is illustrated in Fig. 6 for 100% NF_3 and a rf current of an A. The pressure range was between 80 and 250 mTorr, except for doped poly-Si where only up to 150 mTorr was employed. The same increasing order in etch rate—SiO_2, Mo, $MoSi_2$, and doped poly-Si—is observed. The etch rate of molybdenum exhibited a rather weak functional relationship with pressure when compared to those of SiO_2, $MoSi_2$, and poly-Si. The Mo etch rate ranged between 1800 and 2500 Å/min. In contrast, that of doped poly-Si showed a fairly strong functional relationship, jumping from 0.85 μm/min at 80 mTorr to 2.2 μm/min at 150 mTorr. The pressure dependence of the silicide etching was intermediate to the former two in that, between 80 and 125 mTorr, the etch rate increased sharply with pressure but beyond 150 mTorr, it started to be less dependent and leveled off. In the case of thermal oxide, the etch rate increased monotonically with pressure, ranging between 610 and 1220 Å/min.

Since the gate material is usually placed on top of a thin gate oxide layer, the ability to pattern the gate without significantly etching the underlying oxide is essential. The etch rate ratio between gate metal and oxide is used to characterize selectivity. The data in Figs. 5 and 6 are plotted in Figs. 7 and 8 in terms of etch rate ratio versus rf current and pressure, respectively. As shown in the figures, the selectivity of doped poly-Si over oxide was fairly high (12.5–24). Also, the etch rate ratio between $MoSi_2$ and SiO_2 varied between 5 and 6.5 within the range of rf current studied at 100 mTorr. Similarly, the Mo to SiO_2 etch rate ratio had also a very weak dependence and was ~ 3. On the other hand, the pressure apparently had a substantial effect on the selectivity of both molybdenum and $MoSi_2$ over thermal oxide. At 1 A, the selectivity of silicide over oxide increased from 4.5 at 80 mTorr to 7.2 at 150 mTorr, then leveled off to 8 at 250 mTorr. In contrast, that of molybdenum over oxide was the highest (~ 3.7) at the lowest pressure but decreased with increasing pressure and reached a minimum (1.6) at the highest pressure.

To determine the effect of addition of inert gases, the etching process was characterized with argon or helium diluted NF_3 plasmas. In particular, the etch rates of Mo and its disilicide were determined for several NF_3/Ar and NF_3/He percentages (from 10/90 to 100/0).

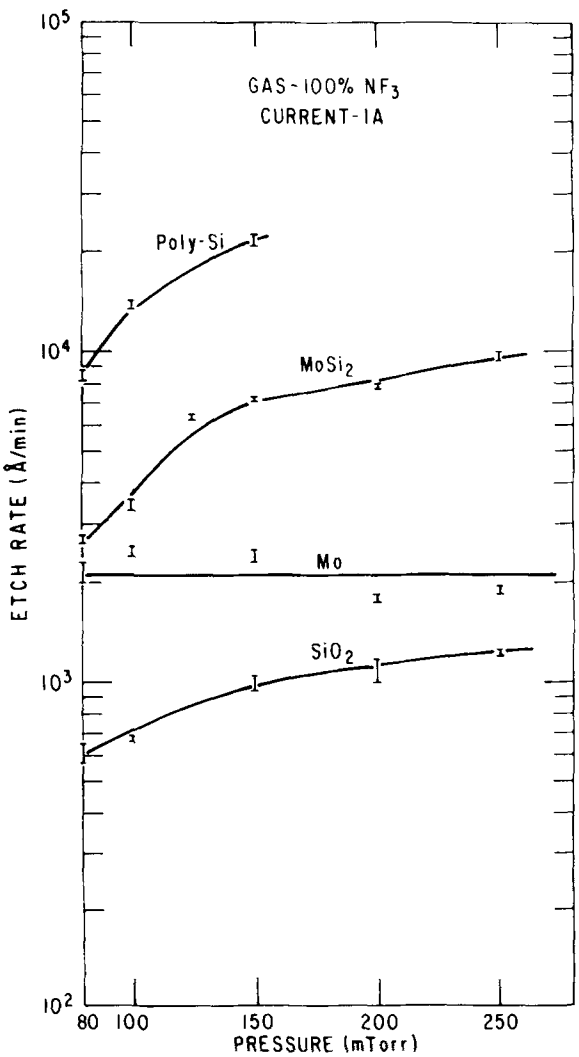

FIG. 6. Etch rates of Mo, $MoSi_2$, doped poly-Si, and SiO_2 are shown as a function of reactor pressure at 1 A in 100% NF_3.

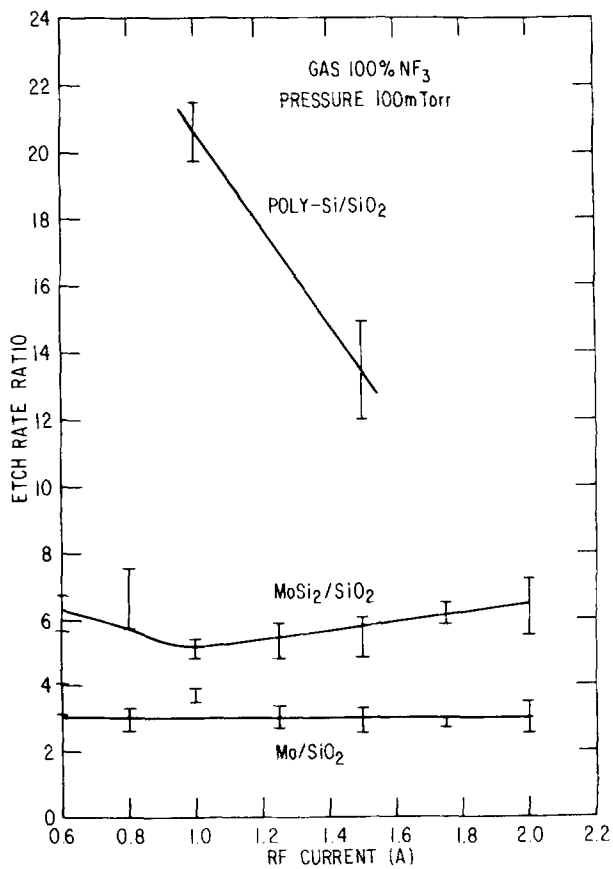

FIG. 7. Etch rate ratios (selectivity) of Mo over SiO_2 and $MoSi_2$ over SiO_2 are shown vs rf current in 100% NF_3 at 100 mTorr.

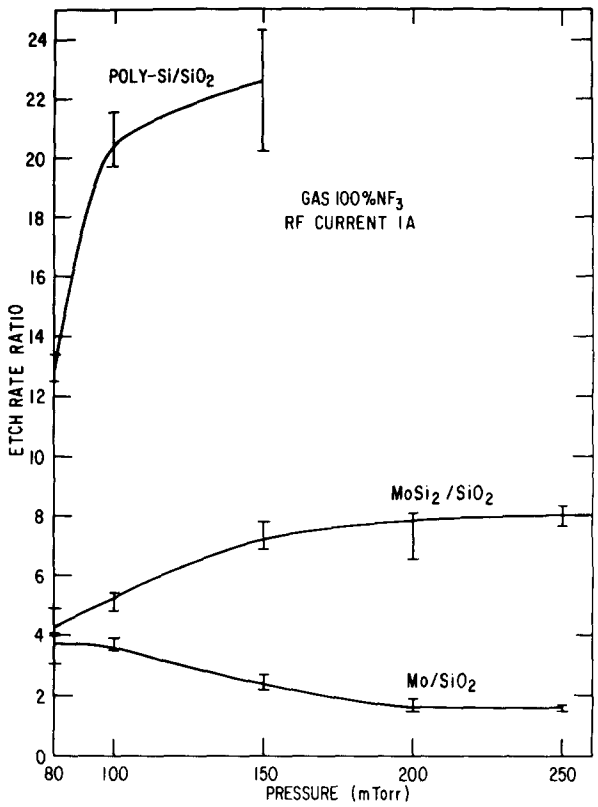

FIG. 8. Etch rate ratios between Mo and SiO_2 and between $MoSi_2$ and SiO_2 are shown vs pressure in 100% NF_3 at 1 A.

In Fig. 9, the etch rates of molybdenum and silicon dioxide are shown for rf current ranging between 0.75 and 2 A at 200 mTorr in a 10% NF_3 plasma diluted with argon. Molybdenum was being etched at a rate of 280 Å/min at 1 A and 440 Å/min at 2 A, while the corresponding oxide etching rates were 130 and 160 Å/min. The functional relationship of both Mo and SiO_2 etch rates and rf current was approximately linear, with a selectivity between 2.2 and 2.8.

The effect of diluting NF_3 with argon and helium in the case of 20% NF_3 and 80% of argon or helium at 200 mTorr and 1 A is shown in Fig. 10. In all cases, the etch rates in 100% NF_3 were higher than either dilution case. In particular, the etch rate of molybdenum decreased from 1800 Å/min to 540 and 790 Å/min when the plasma was 80/20 NF_3/Ar and NF_3/He, respectively; whereas the corresponding silicide etch rate dropped from 7850 Å/min to 1130 and 850 Å/min. The etch rate of thermal oxide also showed marked decrease. The etch rate of doped poly-Si was 3570 Å/min in 20/80 NF_3/Ar but only 1720 Å/min in NF_3/He mixture of the same ratio. Due to the exceedingly fast etching of poly-Si, we have only determined its etch rate in 100% NF_3 up to a pressure of 150 mTorr. Even at this lower pressure, a value of 2.2 μm/min was measured, much higher than those obtained in the diluted plasmas.

Figure 11 illustrates the etch rate change with the percentage of argon in NF_3 between 0% and 90% at a pressure of 200 mTorr and a current of 1 A. The general trend of decreasing etch rate with increasing argon can be readily observed. Specifically, the silicide etch rate decreased from 7850 Å/min with 0% argon to 1130 Å/min with 80% ar-

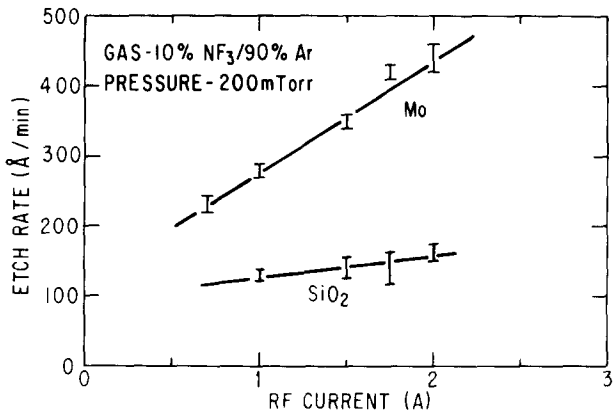

FIG. 9. Etch rates of Mo and SiO_2 vs rf current in 10% NF_3/90% Ar at 200 mTorr.

gon/20% NF_3, while the corresponding Mo etch rate dropped from 1800 to 540 Å/min. Diluting the NF_3 concentration further to 10% resulted in a Mo etch rate of 280 Å/min. Also, the oxide rate varied between 130 Å/min in 10/90 NF_3/Ar and 1090 Å/min in 100% NF_3. It may be noted that an lower than expected etch rate was measured for 50/50 NF_3/Ar. The reason for this deviation has not yet been determined. Doped poly-Si was etched at 1010 Å/min in 10/90 NF_3/Ar but increased rapidly to 1.2 μm/min in 50/50 NF_3/Ar.

The etch rate of the positive photoresist used has not been studied systemically but typical values of 750–3000 Å/

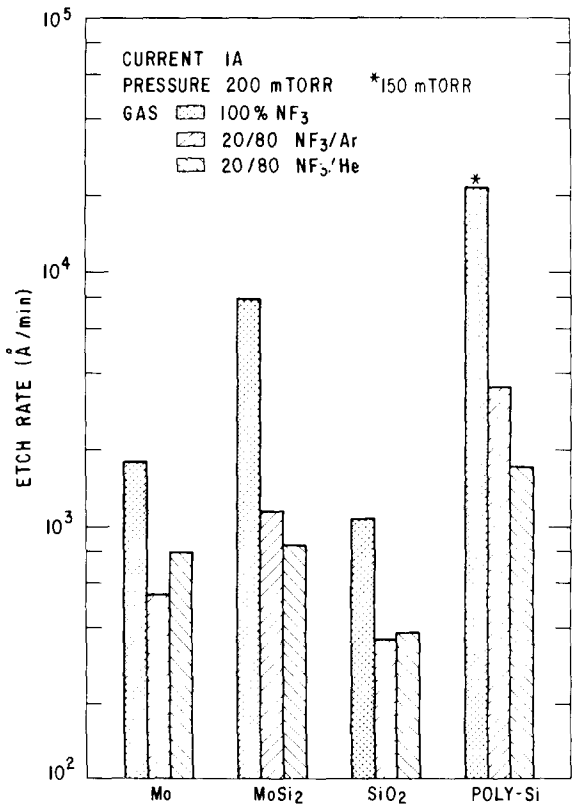

FIG. 10. Etch rates of Mo, $MoSi_2$, SiO_2, and doped poly-Si obtained in 100% NF_3 are compared with those in 20/80 NF_3/Ar and 20/80 NF_3/He. A rf current of 1 A and a pressure of 200 mTorr were used.

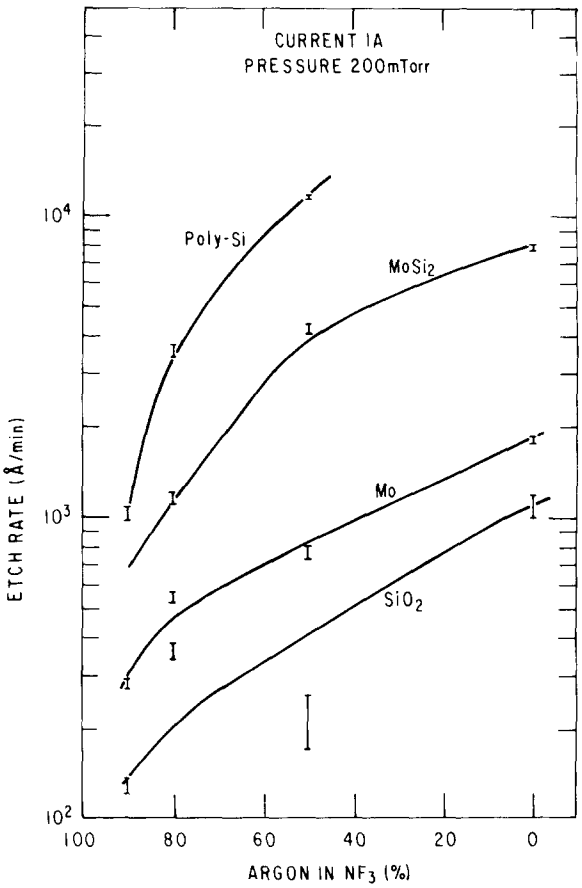

FIG. 11. Etch rates of Mo, $MoSi_2$, doped poly-Si, and thermal oxide are shown as a function of argon percentage in NF_3 at 1 A and 200 mTorr.

min were measured.

The dc voltage on the rf electrode was measured under various conditions. Its dependence on rf current at 100 mTorr in NF_3 is shown in Fig. 12 for the various materials considered here. For $MoSi_2$, it increased from -62 to -90 V when the current varied from 0.6 to 2.0 A. The corresponding range for molybdenum was between -34 and -70 V. A higher range can be seen for oxide and poly-Si etching.

The variation of dc voltage with pressure is illustrated in Fig. 13. Generally, it was much higher below 150 mTorr than above it. For the disilicide, it dropped from -125 to -22 V when the pressure changed from 80 to 125 mTorr. Beyond 125 mTorr, the change was small. A very similar relationship has also been observed for thermal oxide and molybdenum. Moreover, for doped poly-Si, it also decreased from -125 to -25 V between the pressure range of 80–150 mTorr. From these measurements, we can conclude that, below 150 mTorr, there is a higher degree of ion bombardment on all the surfaces in the chamber than above that pressure for all the etching we investigated here.

For the diluted plasmas, generally, a much higher (by as much as an order of magnitude) dc voltage has been measured. Also, the dilution of NF_3 with helium usually resulted in a higher voltage than with argon. For instance, when etching the disilicide at 1 A and 200 mTorr, the dc bias was -20 V for 100% NF_3 but was -57 for 20/80 NF_3/Ar. The corresponding values for etching Mo were -7.5 and -55 V, while those for etching thermal oxide were -10.5 and -55 V, respectively. Furthermore, when etching SiO_2 at 2 A and 100 mTorr in 20/80 NF_3/He, the highest voltage (-670 V) was measured, considerably higher than those in 20/80 NF_3/Ar and 100% NF_3 (-295 and -90 V, respectively).

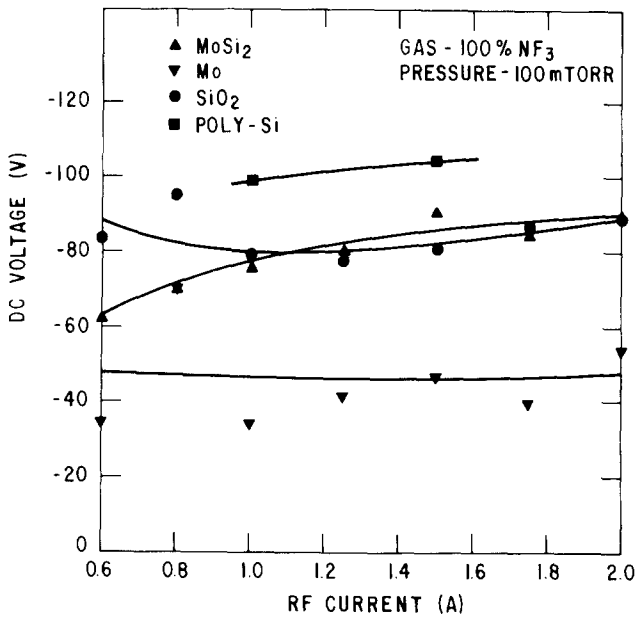

FIG. 12. dc voltage measured on the excitation electrode vs rf current during the etching of Mo, $MoSi_2$, doped poly-Si, and SiO_2 in 100% NF_3 at 100 mTorr.

It should be pointed out that measurements of the rf electrode potential relative to ground were used to give only an indirect measure of the trend of the generally higher potential difference between the plasma and the substrate.[24] The plasma potential was not directly measured.

IV. DISCUSSION

The control of the etching characteristics, such as anisotropy and selectivity, described in the last section requires an understanding of the basic mechanisms of the plasma

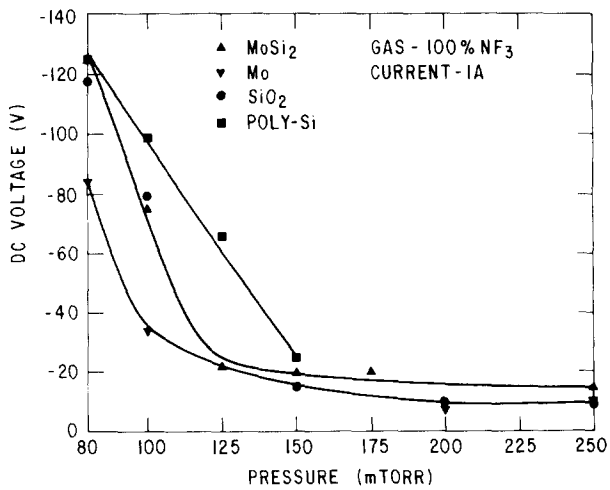

FIG. 13. dc bias vs pressure during the etching of Mo, $MoSi_2$, doped poly-Si, and SiO_2 in 100% NF_3 at 1 A.

etching process. Towards that end, the various reaction steps that take place need to be examined in detail. The sequence of reactions that has been proposed[25] is: (1) nondissociative adsorption of the etching gas molecules at the solid surface being etched, (2) dissociation of these adsorbed molecules, (3) formation of the product molecules from reactions between the adsorbed atoms and the solid surface, (4) desorption of these product molecules into the gas phase, and (5) removal of nonreactive residue, if any, from the surface. Any of these could be the rate-limiting step.[25] Also, many of these events depend critically on the degree of electron and/or ion bombardment. Hence, the interactions of ions, electrons, and neutral radicals with solid surfaces play an important role in these plasma processes.

Detailed examinations of many of these steps have been carried out in the etching of silicon with CF_4-based[10,11,25,26] and, to a lesser extent, SF_6-based[27] plasmas. In contrast, very little work has been reported on NF_3 plasmas.[27,28] Also, while plasma etching of silicon and silicon dioxide has been widely investigated, little information has been published on refractory metal or metal silicide etching. In the following discussion, we will compare these reaction events in CF_4 and NF_3 plasmas for Si, Mo, and $MoSi_2$. In particular, the analysis concentrates on the surface examination of partially etched and unetched (control) Mo and $MoSi_2$ samples using AES. Also, measurements on the dc voltage of the cathode will be discussed with respect to the etching characteristics.

In the case of CF_4, the adsorption and dissociation on the surface of silicon has been attributed to, first, the adsorption of the CF_4 molecule and then its dissociation into various fragments on the solid surface assisted by external radiation.[10,25] The predominant fragments, as detected by mass spectrometry of the effluent, appear to be CF_3 and F.[10,11] Nevertheless, all of the CF_x ($x = 1,2,3$) species are expected to participate in subsequent reactions. No dissociative adsorption has been observed in the absence of external radiation. On the other hand, in the case of XeF_4, dissociative adsorption has been found to take place on silicon surfaces even without a plasma.[29] Finally, in the case of NF_3, we believe the adsorption behavior to resemble that of CF_4 rather than that of XeF_4 since no etching reaction has been observed without external radiation. With plasma discharge, NF_3 is dissociated into various NF_x radicals, each of which is expected to contribute fluorine to the etching process. The NF_3 plasma differs somewhat from a CF_4 plasma in that uncracked parent molecules have also been detected,[29,31] even though NF_2, the counterpart of CF_3, is still the major species.

Next, the dissociated radicals readily react with the solid surface to form fluorinated compounds. For silicon, SiF_4 has been found to be the ultimate reaction product in CF_4, as well as many other fluorine-based plasmas.[10,11,26,27] Thus, we do not expect NF_3 etching of silicon to deviate from this trend. For molybdenum, MoF_6 has been reported in plasma etching with CF_4.[32] It is very likely that the same products are formed in molybdenum silicide etching, though this assertion has not yet been verified experimentally.

The desorption of these product molecules from the solid surface is the third important event. The desorption rate depends on, among other things, vapor pressure of reaction products and gas flow. Due to the volatile nature of SiF_4 (vapor pressure over 20 atm at room temperature[33]), its desorption is not a problem after its formation. In contrast, MoF_6 has a vapor pressure of only 400 Torr at 290 °K.[34] Thus, its limited desorption can slow further reactions from proceeding. Also, in contrast to CF_4, all of the constituents of NF_3 are gases at room temperature. Thus, no solid residue (e.g., carbon) is left on the etched surface.

To examine the etched surface, Auger analysis was performed on Mo and $MoSi_2$ samples before and after NF_3 etching. The Auger spectra for molybdenum films which were partially etched in 100% NF_3 and unetched (control) are shown in Fig. 14. In Fig. 14(a), the as is surface of the partially etched sample is analyzed. Besides carbon and oxygen, both of which are always present on air-exposed surfaces, molybdenum, fluorine, nitrogen, and possible traces of titanium were detected. Ion milling the surface with argon for 3 min (removing ~ 75 Å) eliminated most of the oxygen and some of the carbon [Fig. 14(b)]. The rest of the carbon in the film originated from the sputtering target, as verified in the bulk of the unetched sample [compare Fig. 14(b) with Fig. 14(d)]. Also, the Auger line shapes of surface and bulk carbon indicate the latter was chemically bonded while the former was not. Fluorine was no longer present, pointing out that it was confined to the surface. The controlled sample surface [Fig. 14(c)] showed similar amounts of oxygen and carbon but exhibited a much smaller amount of nitrogen, indicating that the nitrogen originated from the plasma.

The Auger spectra for partially etched and unetched $MoSi_2$ films are illustrated in Fig. 15. The unetched sample surface showed oxygen, carbon, and silicon but only a negligible amount of molybdenum [Fig. 15(d)]. Ion milling the sample for 3 min eliminated most of the oxygen and carbon but detected, as expected, a significant amount of molybdenum [Fig. 15(e)]. This shows that the silicide surface is usually covered with a thin layer of native oxide (SiO_x) which is highly metal deficient. The as is surface of the partially etched sample was very different [Fig. 15(a)]. In addition to oxygen and carbon, fluorine, molybdenum, and nitrogen, as well as trace amounts of titanium, iron, and aluminum were detected. No silicon was observed on the surface. Ion milling for 3 min [Fig. 15(b)] increased the silicon and molybdenum peaks but reduced the intensity of the other peaks. Finally, after ion milling for 15 min [Fig. 15(c)], most of the contaminants decreased to noise level except for oxygen and carbon. The similar presence of these last two in both samples [Figs. 15(c) and 15(e)] probably indicates their level in the sputtering target. The presence of molybdenum but not silicon on the etched surface points to the limited desorption of molybdenum compounds (probably MoF_6) but not silicon compounds (SiF_4). This is consistent with the significantly higher vapor pressure of SiF_4 vs MoF_6. The role of nitrogen on the surface is still unclear. It may participate in some surface reactions not yet identified. All of the other contaminants can be traced to either the sputtering target (oxygen and carbon) or the reactor chamber or electrode

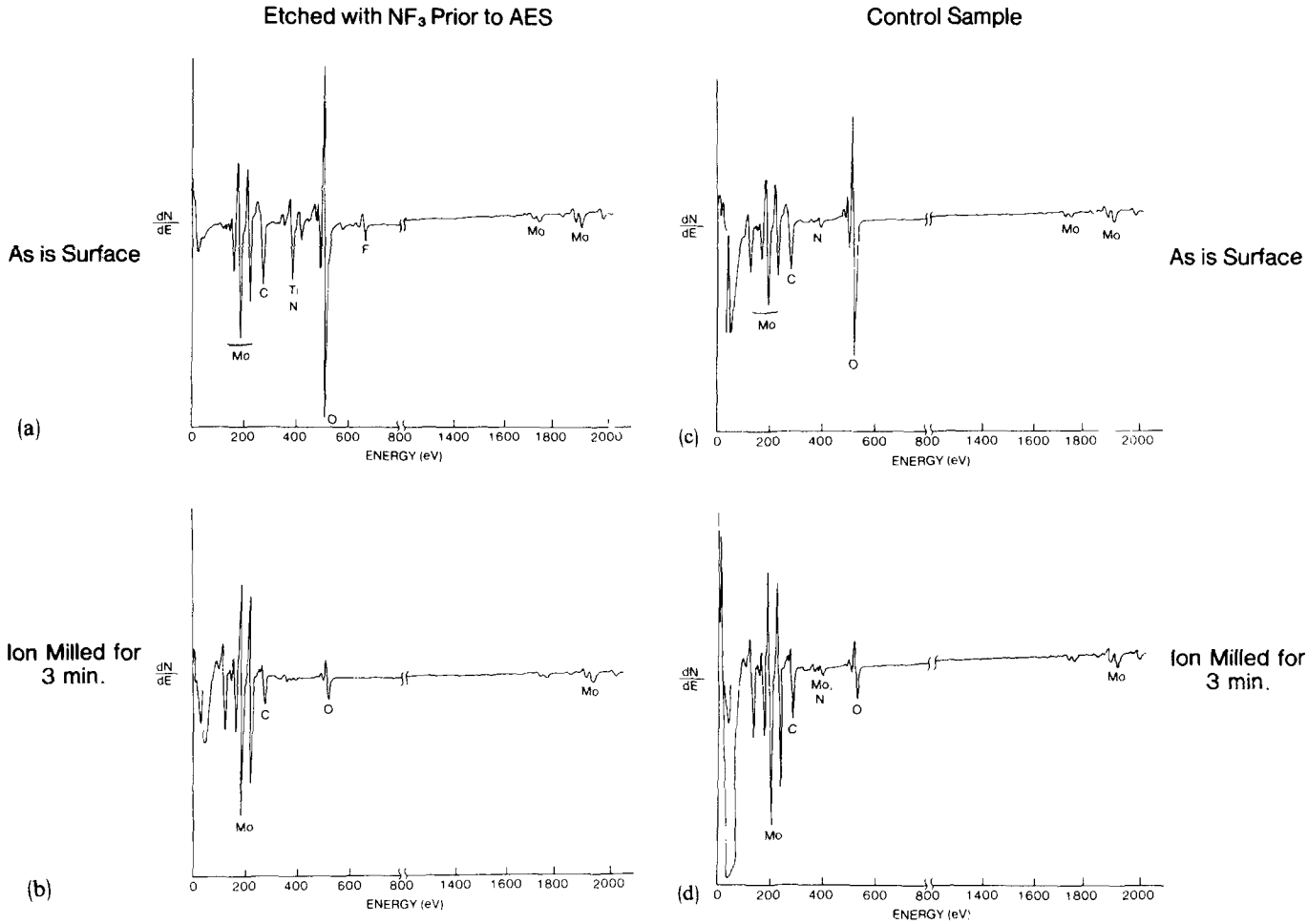

FIG. 14. Auger spectra for partially etched and unetched (control) molybdenum films: The as is surfaces of the (a) partially etched and (c) unetched samples; the same surfaces after ion milling with argon for 3 min, (b) and (d), respectively.

(aluminum, iron, and titanium).

The increase of the various etch rates with applied current, as shown in Fig. 2, can be due to all the mechanisms above. However, since no large variation of the dc bias on the rf electrode has been measured within the range studied, the dependence of the etch rates on rf current are predominantly chemical in nature. On the other hand, the pressure dependence of the etch rates exhibits different behaviors for the various materials investigated here. For poly-Si, the dependence is very strong. The etch rate of thermal oxide also increases with pressure, but not as strong as that of poly-Si. This is an indication that both of these processes are mass-transfer limited. On the other hand, for molybdenum, the etch rate hardly changes with pressure. This is probably due to the limiting effect of either the surface reaction rate or the desorption rate of the molybdenum compounds formed. In the case of the silicide, the initial etching behavior appears to be mass-transfer limited while at higher pressure (>150 mTorr), it becomes more reaction-rate limited. As to the physical effects, because the dc voltage on the excitation electrode decreases rapidly between 80 and 150 mTorr, the degree of ion bombardment is higher at lower pressures. This factor may explain the lower selectivity of poly-Si and $MoSi_2$ over SiO_2 at lower pressures.

The dilution of NF_3 with either argon or helium uniformly resulted in a lower etch rate under all conditions. It has been pointed out earlier that the dc bias on the rf electrode detected in diluted NF_3 plasmas was much higher than in 100% NF_3. This would indicate a larger degree of ion bombardment in the diluted plasmas. Therefore, the significant decrease in etch rate when NF_3 is diluted with argon or helium can then be attributed to the larger influence of the decrease in concentration of reactants. Consequently, either argon or helium may be used as dilutant for NF_3.

Ion bombardment, as inferred from dc voltage measurements, is stronger in the helium dilution case than in the argon dilution case, resulting in higher etch rates in the former. However, the etch rates measured for 20% NF_3 with 80% argon or 80% helium apparently indicate that the dependence of etch rate on ion bombardment is more complex because the etch rate is not always higher in the helium diluted plasmas. Also, it is worth noting that the plasma was seen to be less stable with the addition of helium than with argon.

V. SUMMARY

The etching characteristics of Mo and $MoSi_2$ with NF_3 mixtures in a planar plasma reactor has been described and

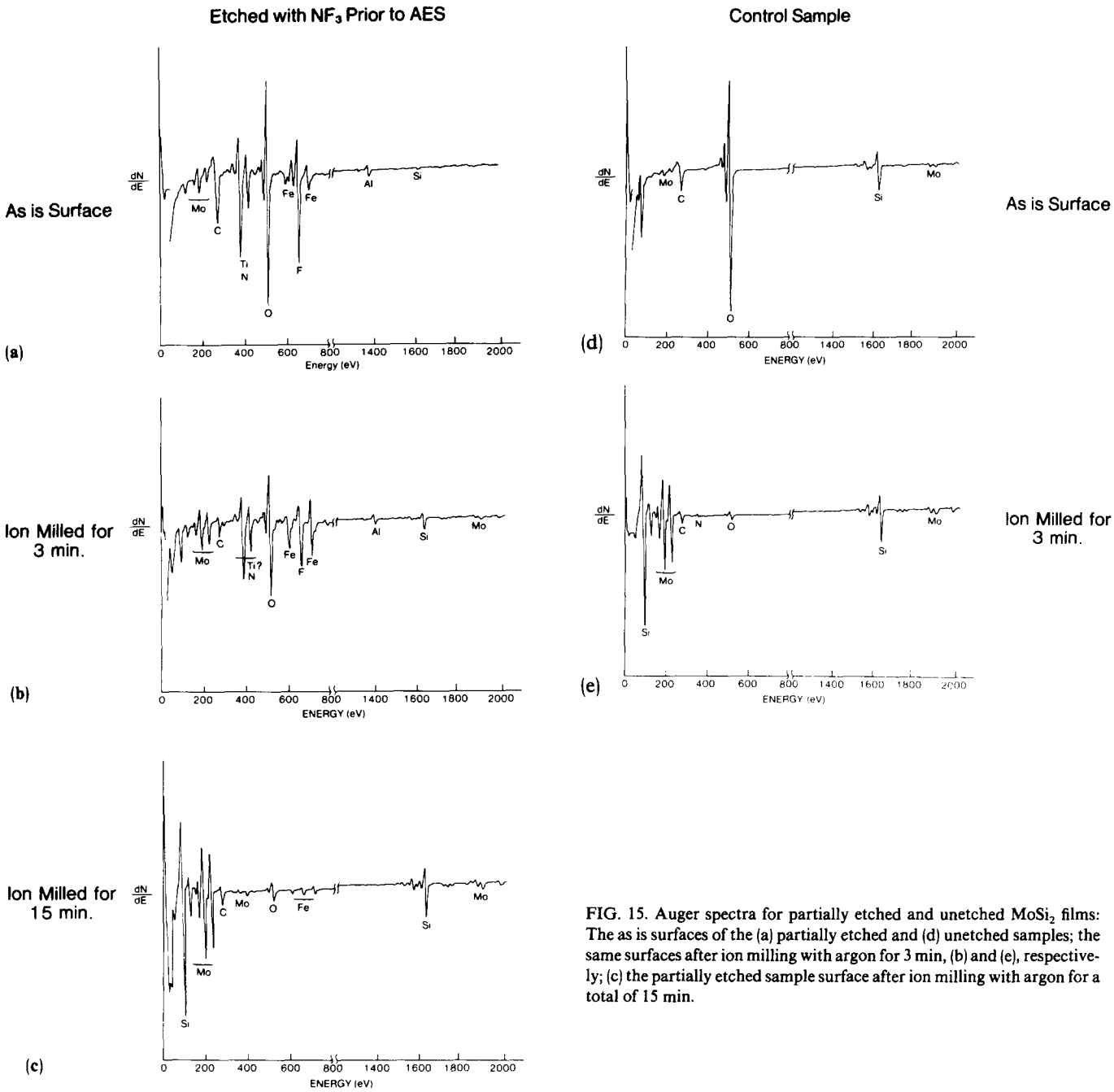

FIG. 15. Auger spectra for partially etched and unetched $MoSi_2$ films: The as is surfaces of the (a) partially etched and (d) unetched samples; the same surfaces after ion milling with argon for 3 min, (b) and (e), respectively; (c) the partially etched sample surface after ion milling with argon for a total of 15 min.

compared with those of phosphorus-doped poly-Si and thermally grown SiO_2. The dependence of etch rate on applied rf current, reactor pressure, and dilution with argon and helium is studied. The selectivity of Mo over SiO_2 and $MoSi_2$ over SiO_2 was found to be 1.5-4 and 4-8 and the anisotropy was ~ 3 for both cases. Measurements of the dc bias on the rf electrode showed that ion bombardment was higher below 150 mTorr and in argon and helium diluted plasmas. Comparative Auger analysis indicated that desorption of molybdenum compounds, but not silicon compounds, can be the rate-limiting step for both metal and silicide etching. The application of this etching process has resulted in successful fabrication of high-resolution Mo and $MoSi_2$ gate devices and circuits.[35,36] Furthermore, silicide structures as small as 1000 Å were also fabricated using an edge-defined technique with a modified version of this process.[37]

ACKNOWLEDGMENTS

The authors would like to thank D. H. Bower, B. A. Heath, and D. M. Brown for many helpful discussions, J. F. Norton and S. Okazaki for the SEM pictures, and K. L. Lanning, C. J. Ludwin, and G. J. Charney for processing assistance. AJS also acknowledges the Office of Naval Research for its partial support of this work.

[1]P. L. Shah, IEEE Trans. Electron Devices **ED-26**, 631 (1979).
[2]H. Ishikawa, M. Yamamoto, H. Tokunaga, N. Toyokura, F. Yanagawa, K. Kiuchi, and M. Kondo, IEEE Trans. Electron Devices **ED-27**, 1586 (1980).
[3]F. Yanagawa, K. Kiuchi, T. Mosoya, T. Tsuchiya, T. Amazawa, and T. Mano, IEEE Trans. Electron Devices **ED-27**, 1602 (1980).
[4]T. Mochizuki, K. Shibata, T. Inoue, and K. Ohuchi, Jpn. J. Appl. Phys. **17**, Suppl. 17-1, 37 (1977).
[5]B. L. Crowder and S. Zirinsky, IEEE Trans. Electron Devices **ED-26**, 369 (1980).
[6]T. P. Chow and A. J. Steckl, Appl. Phys. Lett. **36**, 297 (1980).
[7]S. P. Murarka, J. Vac. Sci. Technol. **17**, 775 (1980).
[8]H. J. Geipel, Jr., N. Hsieh, M. H. Ishaq, C. W. Koburger, and F. R. White, IEEE Trans. Electron Devices **ED-27**, 1417 (1980).
[9]A. K. Sinha, W. S. Lindenburger, D. B. Fraser, S. P. Murarka, and E. N. Fuls, IEEE Trans. Electron Devices **ED-27**, 1425 (1980).
[10]H. F. Winters, J. W. Coburn, and E. Kay, J. Appl. Phys. **48**, 4973 (1978).
[11]C. J. Mogab, A. C. Adams, and D. L. Flamm, J. Appl. Phys. **49**, 3796 (1978).
[12]R. A. Gdula, Electrochem. Soc. Fall Meeting 1979, Extended Abstract **79-2**, 1524 (1979).
[13]C. J. Mogab and H. J. Levinstein, J. Vac. Sci. Technol. **17**, 721 (1980).
[14]D. H. Bower, J. Electrochem. Soc. **129**, 795 (1982).
[15]G. J. Schwartz and P. M. Schaible, J. Vac. Sci. Technol. **16**, 410 (1979).
[16]T. P. Chow and A. J. Steckl, Appl. Phys. Lett. **37**, 466 (1980).
[17]F. R. White, C. W. Koburger, H. J. Geipel, and D. L. Harmon, Electrochem. Soc. Fall Meeting, Extended Abstract **80-2**, 854 (1980).
[18]L. M. Ephrath, IEEE Trans. Electron Devices **ED-28**, 1315 (1981).
[19]T. P. Chow and A. J. Steckl, IEEE IEDM Tech. Dig. 149 (1980).
[20]W. Beinvogl and B. Hasler, Electrochem. Soc. 4th International Silicon Symposium, Extended Abstract, 648 (1981).
[21]K. Hirata, Y. Ozaki, M. Oda, and M. Kimizuka, IEEE Trans. Electron Devices **ED-28**, 1323 (1981).
[22]K. L. Wang, T. C. Holloway, R. F. Pinizzoto, Z. P. Sobczak, W. R. Hunter, and A. F. Tasch, Jr., IEEE IEDM Tech. Dig., 58 (1981).
[23]B. Gorowitz (unpublished).
[24]J. L. Vossen, J. Electrochem. Soc. **126**, 319 (1979).
[25]H. F. Winters, J. Appl. Phys. **49**, 5165 (1978).
[26]E. Kay, J. Coburn, and A. Dilks, *Topics in Current Chemistry, Vol. 94, Plasma Chemistry III*, edited by S. Veprek and M. Venugopalan (Springer, Berlin 1980), p. 1.
[27]R. d'Agostino and D. L. Flamm, J. Appl. Phys. **52**, 162 (1981).
[28]K. M. Eisele, Electrochem. Soc. Spring Meeting, Extended Abstract **80-1**, 285 (1980).
[29]N. J. Ianno, K. E. Greenberg, and J. R. Verdeyen, J. Electrochem. Soc. **128**, 2174 (1980).
[30]T. J. Chuang, J. Appl. Phys. **51**, 2614 (1980).
[31]R. M. Reese and V. H. Dibeler, J. Chem. Phys. **24**, 1175 (1956).
[32]A. Dilks and E. Kay, in *Plasma Polymerization* (ACS Symposium Series 108), edited by M. Shen and A. T. Bell (American Chemical Society, Washington, D. C., 1979), p. 195.
[33]*Handbook of Chemistry and Physics*, 60th ed., edited by R. C. Weast (Chemical Rubber Co., Cleveland, Ohio, 1979), p. D203.
[34]G. H. Cady and G. B. Hargreaves, J. Chem. Soc. 1563 (1961).
[35]T. P. Chow, M. Ghezzo, A. J. Steckl, and D. M. Brown, Electrochem. Soc. Spring Meeting, Extended Abstract **81-1**, 738 (1981).
[36]T. P. Chow, A. J. Steckl, and R. T. Jerdonek, IEEE Electron Dev. Lett. **EDL-3**, 37 (1982).
[37]S. Okazaki, T. P. Chow, and A. J. Steckl, IEEE Trans. Electron Devices **ED-28**, 1364 (1981).